Heliyon 6 (2020) e04143

Contents lists available at ScienceDirect

Heliyon

journal homepage: www.cell.com/heliyon

Research article

A method for reducing animal use whilst maintaining statistical power in electrophysiological recordings from rodent nerves

Laura R. Rich [a], Jonathan A. Patrick [a], Margaret A. Hamner [b], Bruce R. Ransom [b], Angus M. Brown [a,b,*]

[a] School of Life Sciences, University of Nottingham, Nottingham, NG2 5HY, UK
[b] Department of Neurology, University of Washington School of Medicine, Box 356465, 1959 Pacific Ave NE, Seattle, WA 98195, USA

ARTICLE INFO

Keywords:
Neuroscience
Statistics
Mathematical analysis
Nervous system
Electrophysiology
Molecular neuroscience
Compound action potential
Power
Hypothesis testing
Error
Microsoft excel
Nerve trunk
ex vivo

ABSTRACT

The stimulus evoked compound action potential, recorded from *ex vivo* nerve trunks such as the rodent optic and sciatic nerve, is a popular model system used to study aspects of nervous system metabolism. This includes (1) the role of glycogen in supporting axon conduction, (2) the injury mechanisms resulting from metabolic insults, and (3) to test putative benefits of clinically relevant neuroprotective strategies. We demonstrate the benefit of simultaneously recording from pairs of nerves in the same superfusion chamber compared with conventional recordings from single nerves. Experiments carried out on mouse optic and sciatic nerves demonstrate that our new recording configuration decreased the relative standard deviation from samples when compared with recordings from an equivalent number of individually recorded nerves. The new method reduces the number of animals required to produce equivalent Power compared with the existing method, where single nerves are used. Adopting this method leads to increased experimental efficiency and productivity. We demonstrate that reduced animal use and increased Power can be achieved by recording from pairs of rodent nerve trunks simultaneously.

1. Introduction

Application of the suction electrode technique to record the stimulus evoked compound action potential (CAP) from rodent nerve trunks was introduced in the late 1980s (Baker et al., 1987; Kocsis et al., 1986) and subsequently adopted to assess the damage incurred by central white matter as a result of metabolic insult (Fern et al., 1994; Ransom and Fern, 1997; Stys et al., 1992). However the technique can also be applied to record the CAP from peripheral nerve (Brown et al., 2012; Rich and Brown, 2018). The CAP area represents the best measure of the number of active axons since currents generated by individual axons within a fibre tract sum linearly (Cummins et al., 1979; Stys et al., 1991). Thus the ratio of the post-insult CAP area to pre-insult baseline provides a quantitative index of tissue injury (Stys et al., 1991) that can be used to assess any benefits of neuroprotective intervention (Stys et al., 1990). The physiological processes that this versatile technique have been applied to include, but are not limited to, (1) the role of glycogen in supporting axon conduction in both central (Brown et al., 2003) and peripheral nerve (Brown et al., 2012), (2) the efficacy of energy substrates in supporting axon conduction (Brown et al., 2001; Rich and Brown, 2018), (3) the consequences of demyelination (Edgar et al., 2009, 2010), and (4) retinal ischemia (Wang et al., 2012).

The initial description of suction electrode recordings used only a single optic nerve from each animal, its partner being discarded (Stys et al., 1991). In more recent studies both optic nerves have been placed in the same superfusion recording chamber and paired sets of stimulating and recording electrodes used to acquire CAPs from both nerves simultaneously (Hamner et al., 2011). This method has obvious advantages in studies such as investigations into the effects of ischaemic pre-conditioning on subsequent CAP recovery in optic nerves exposed to oxygen glucose deprivation (OGD), where surgical occlusion of the blood supply to one optic nerve was compared with its untreated partner nerve (Hamner et al., 2015).

The mouse sciatic and optic nerves have both served as models to assess the role of glycogen in supporting axon conduction during periods of metabolic stress (Brown et al., 2003, 2012; Rich and Brown, 2018). The stimulus evoked A fibre CAP in sciatic nerve is maintained for many hours when superfused with aCSF containing 10 mM glucose, however

* Corresponding author.
E-mail address: ambrown@nottingham.ac.uk (A.M. Brown).

https://doi.org/10.1016/j.heliyon.2020.e04143
Received 13 November 2019; Received in revised form 21 November 2019; Accepted 2 June 2020

upon removal of glucose from the aCSF, simulated aglycaemia, the CAP starts to fall after about 90 min, totally failing by 200 min (Rich and Brown, 2018). Based on experiments carried out in mouse optic nerve (MON) (Brown et al., 2003) we hypothesize that increasing the tissue energy demand in sciatic nerve by imposing 50 Hz stimulus during aglycaemia will attenuate the latency to A fibre CAP failure, since the increased metabolic demand will accelerate consumption of Schwann cell glycogen, which supports A fibre axon conduction in the absence of exogenously applied glucose (Brown et al., 2012). These experiments provided the raw data from which we derived a mathematically based rationale that supports recording from pairs of nerves in the same superfusion chamber. The new recording method reduces experimental variability i.e. random error, and demonstrates that statistical power can be maintained whilst reducing animal use.

2. Material and methods

2.1. Ethical approval

All experiments were approved by the University of Nottingham Animal Care and Ethics Committee, and were carried out in accordance with the Animals (Scientific Procedures) Act 1986 under appropriate authority of establishment, project and personal licences. Experiments were performed on male CD-1 mice (weight 28–35 g, corresponding to 30–45 days of age) purchased from Charles River Laboratories (Margate, Kent, CT9 4LT, UK). Mice were group housed with *ad libitum* access to food and water, and maintained at 22–23 °C on a 12:12 h light-dark cycle. Mice were sacrificed by Schedule 1 cervical dislocation followed by decapitation.

2.2. Electrophysiological recordings

Details of the dissection of the sciatic nerves (Rich and Brown, 2018) and optic nerves (Brown et al., 2003) have been described in detail previously. The nerves were allowed to equilibrate in the interface superperfusion chamber (Medical Systems Corp, Greenvale, NY), for 30 min prior to recording. The nerves were maintained at 37 °C and superfused with aCSF containing (in mmol/L): NaCl 126, KCl 3.0, $CaCl_2$ 2.0, $MgCl_2$ 2.0, NaH_2PO_4 1.2, $NaHCO_3$ 26 at a rate of about 2 ml min^{-1}. Control aCSF contained 10 mM glucose. The chamber was continuously aerated by a humidified gas mixture of 95% O_2/5% CO_2. Suction electrodes back-filled with the appropriate aCSF were used for stimulation and recording. One electrode was attached to each end of the nerve to record the compound action potential (CAP), thus recordings from the optic nerves were orthodromic. We employed two separate recording set ups, a conventional one in which single nerve CAPs were recorded (Brown et al., 2003; Rich and Brown, 2018), and a set up where pairs of nerves were recorded simultaneously in the same superfusion chamber (Figures 3A and 4A). The experimental protocol involved stimulating nerves continuously at a rate of 1 Hz during the baseline period, followed by a period of aglycaemia, during which nerves were stimulated at either 1 Hz or 50 Hz. A Grass S88 double channel stimulator was used to generate a stimulus of 30 μs duration, and its amplitude adjusted to evoke the maximum CAP possible and then increased another 25% (i.e. supramaximal stimulation, Stys et al., 1991). The stimulus artefact was subtracted as previously described (Rich and Brown, 2018). The signal was amplified up to x1000 in AC mode by a Stanford Research Systems Preamplifier, low pass filtered at 30 kHz (SR560, Stanford Research Systems, Sunnyvale, CA), subsequently digitized at 20 kHz via a Digidata 1400 A/D board, recorded using PClamp 10.7 and analysed with Clampfit 10.7 (Molecular Devices, Wokingham, UK). Optic nerve axon conduction was monitored quantitatively as the area under the supramaximal CAP (Brown et al., 2003) whereas the amplitude of the sciatic nerve A fibre CAP was considered the best measure of the number of active A fibre axons (Patton, 1982; Rich and Brown, 2018).

2.3. Bootstrapping

Bootstrapping involves estimating variation within the dataset by creating smaller datasets from the larger sample, and re-estimating the location and spread of the data. By repeating this process (reselecting data from the dataset and performing the analyses on the new, smaller dataset) many times, it provides a more precise estimate of the true value (Curran-Everett, 2009b). Here, bootstrapping was used to estimate the relative standard deviation (RSD) of the latency of n nerves. For each value of n, the latency of n nerves was selected from the dataset at random. The sample mean (X) and sample standard deviation (S) for the new sample dataset were calculated, from which a new estimate of the RSD (RSDs) could be produced. This process was repeated 1000 times to generate a large set of $\overline{X}$, and RSDs. The mean and SD of the set of $\overline{X}$ provides a robust calculation of the population RSD (RSDp). The set of RSDs is ordered from lowest to highest; the confidence interval of RSDp is provided by values of the 50th and 950th RSDs in this set.

2.4. Data analysis

Data are expressed as the mean ± standard deviation unless otherwise stated. All data manipulation and simulations were carried out using Microsoft Excel (Microsoft Corp, Redmond, WA, USA). Statistical tests were carried out with Prism 7 (GraphPad Software, San Diego, CA). The curve fitting routine for detecting latency to CAP failure has previously been described (Brown, 2006; Wender et al., 2000).

3. Theory

Hypothesis testing is central to the role of statistical analysis. The null hypothesis (H_0) states that there is no real difference between the test and control data i.e. H_0: $\mu_1 = \mu_2$, where μ_1 and μ_2 represent the means of the two populations, whereas the alternate hypothesis (H_1) states that a real difference does indeed exist between the test and control data, i.e. H_1: $\mu_1 \neq \mu_2$ (Bernstein and Bernstein, 1999; Curran-Everett, 2009a; De Muth, 2006; Motulsky, 1995; Sokal and Rohlf, 1995). The risk of making a Type I error is the determining factor in acceptance or rejection of H_0 (Bernstein and Bernstein, 1999). This concept is illustrated graphically in Figure 1A and shows that if $p > \alpha$ then the risk of a Type I error is too great and we fail to reject the H_0 hypothesis. Introducing test data (upper distribution), whose population mean is μ_2, illustrates the concept of the Type II error, which is the risk of failing to reject H_0, when it is in fact false. The area of the test distribution to the right of the *critical value* is defined as β, the risk of making a Type II error. The relationship illustrated in Figure 1A can be expressed in algebraic form as:

$$z_\beta = \frac{\mu_1 - \mu_2}{\sigma} - z_\alpha \quad (1)$$

where z_β is a standard deviation-based value that can be converted to a probability (area under the curve) based on the standard normal distribution, and determines the value of β. The magnitude of β, the Type II error, can also provide information on Power, defined as the complement of β, which is calculated as:

$$\text{Power} = 1 - \beta \quad (2)$$

The Power of a study expressed as a percentage, i.e. (1 - β) *100, usually stated as 80%, is defined as the probability that a statistical test will detect a significant difference when it exists. Power can be visualised as the area of the test distribution that lies to the left of the *critical value* in Figure 1A. The sharp fall in Power as μ_2 approaches μ_1 clearly indicates that it is easier to detect differences between samples groups when the effect size is large (Figure 1B). The data illustrated in Figs 1B, C can be combined to show the reciprocity between effect size and n on Power (Figure 1D). In order to determine the optimal effect size for a desired Power and known value of n, Eq. (1) can be rearranged as:

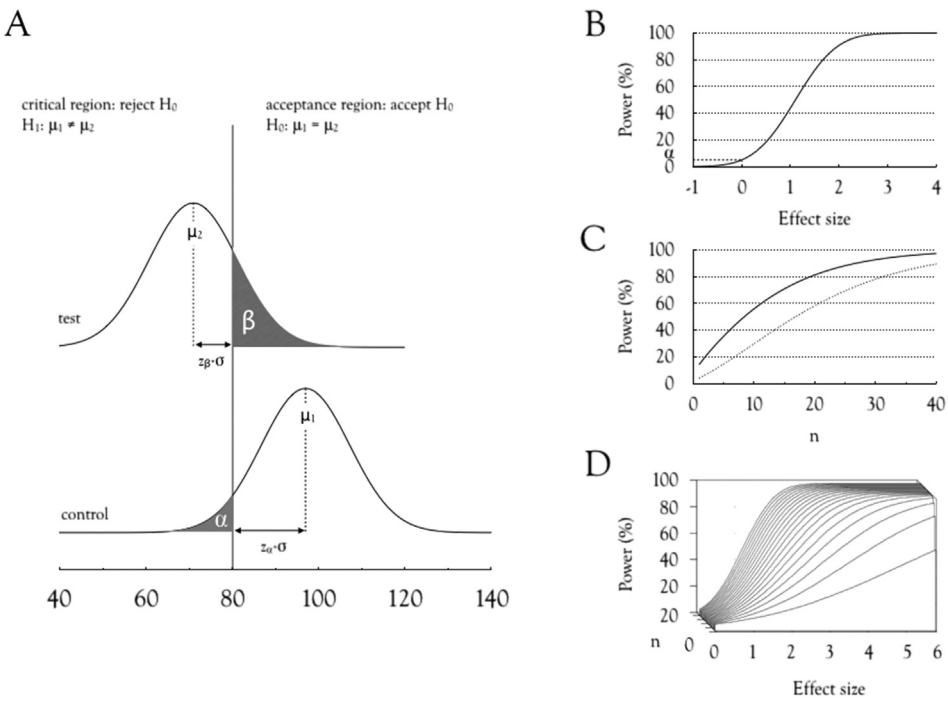

Figure 1. The risk of Type I and Type II errors in a one-tailed test. A. The control population is expressed as a normalised distribution function (lower), whose profile is determined by the mean ± σ, 97.0 ± 29.0. The critical value of the test is indicated by the continuous vertical line and is calculated as the mean of the control distribution (μ_1) minus z_α, where $\alpha = 0.05$. Thus the chance of making a Type I error is denoted by the shaded area of the control distribution (α) to the left of the *critical value*. The test data (upper distribution) has a mean (μ_2) of 71.0, smaller than that of the control distribution i.e. $\mu_2 < \mu_1$, but the same σ. The area of the test distribution to the right of the *critical value* (β) denotes the chance of making a Type II error. Thus α and β are inversely related to each other, as one increases so the other decreases. B. As the magnitude of the effect size increases so does the power, where $\sigma = 3$, $n = 20$ and $\alpha = 0.05$. C. Increasing the value of n causes an increase in power that is more pronounced at $\alpha = 0.05$ (continuous line) than at $\alpha = 0.01$ (dotted line). D. Likewise increasing n causes a decrease in β that is greater when $\alpha = 0.05$ (continuous line) than at $\alpha = 0.01$ (dotted line). For B and C $\sigma = 3$ and the effect size is 1.7. The complementary nature of β and power is clearly visible. D. Power expressed as a function of effect size and sample size, n, where $\sigma = 3$ and $\alpha = 0.05$.

$$n = \frac{SEM^2}{(\mu_1 - \mu_2)}(z_\alpha + z_\beta)^2 \quad (3)$$

which returns the relationship required to calculate the number of samples for a known effect size and SEM. Unfortunately this relationship is not easy to solve since the SEM varies with n. However the built-in function Solver in Excel is capable of carrying out the complex iterative calculations required to solve for n. Figure 2A, B illustrates a table representing the spreadsheet template we use in such power calculations.

4. Results

Increasing the stimulus frequency to 50 Hz accelerated A fibre CAP failure during aglycaemia (Figure 3B), which was assessed as the latency for the CAP to fall to 95% of its baseline value (Figure 3B, Wender et al., 2000). Displaying the data as normalised distributions whose profile is determined by the mean and SD allows a visual comparison between the data acquired with single or pairs of nerves (Figure 3C). In recordings from single nerves (Figure 3Ca) stimulated at 1 Hz, the mean latency to CAP failure was 99.4 ± 28.0 min (n = 12) versus 79.7 ± 24.9 min (n = 12) for nerves stimulated at 50 Hz, a significant difference (p = 0.040: two sample unequal variance t-test). In recordings from pairs of nerves the equivalent values were 96.4 ± 17.2 min (n = 12) versus 80.1 ± 18.9 min (n = 12), p = 0.019. There was no significant difference between the mean values for nerves stimulated at 1 Hz or 50 Hz in pairs or single nerves (p = 0.40 and 0.41, respectively). Although the mean values were similar between each set up, the standard deviation was decreased in recordings from pairs of nerves compared to single nerve recordings, reflected in a narrower distribution; compare the distributions for 1 Hz pair and 1 Hz single (Figure 3C). This difference can be more accurately reported as the relative standard deviation (RSD), which is the coefficient of variation (S/x) expressed as a percentage. We illustrate this by

A

	A	B	C
1	Solve for n		
2			
3	μ_1	100	
4	μ_2	105	
5	SEM	8.944	=(B6/(B7^0.5)
6	SD	20	
7	n	5	
8	n	5	=roundup(B7,0)
9			
10	β	0.288	=normdist(B3,B4,B5,true
11			
12	power	71.19	=(1-B10)

B

	A	B
1	Solve for n	
2		
3	μ_1	100
4	μ_2	105
5	SEM	5.941
6	SD	20
7	n	11.333
8	n	12
9		
10	β	0.200
11		
12	power	71.19

Figure 2. The Excel spreadsheet template used to facilitate power calculations. A. The initial operation requires populating the spreadsheet with realistic values based on experimental data. These data are labelled in Column A, the values are given in Column B, and where appropriate the equations required to determine the data illustrated in the corresponding row in Column C. In this particular instance the values of μ_1 and μ_2 are 100 and 105, respectively, with the SD = 20 and the SEM calculated as $SD/\sqrt{n}$. The value of β, calculated using the normdist function, is 0.288, corresponding to a power of 71.2%. Once the data are input Solver is opened and the Objective cell (β) set at a value of 0.2, i.e. power of 80% is desired, by changing the value of n. Activating Solver begins the iterative process by which the optimal value of n is calculated, whilst maintaining β at 0.2. Note that the value of n is rounded up. B. The solution illustrating that n of 12 is required to achieve a power of 80% based on the input variables. The function Goal Seek can carry out equivalent calculations.

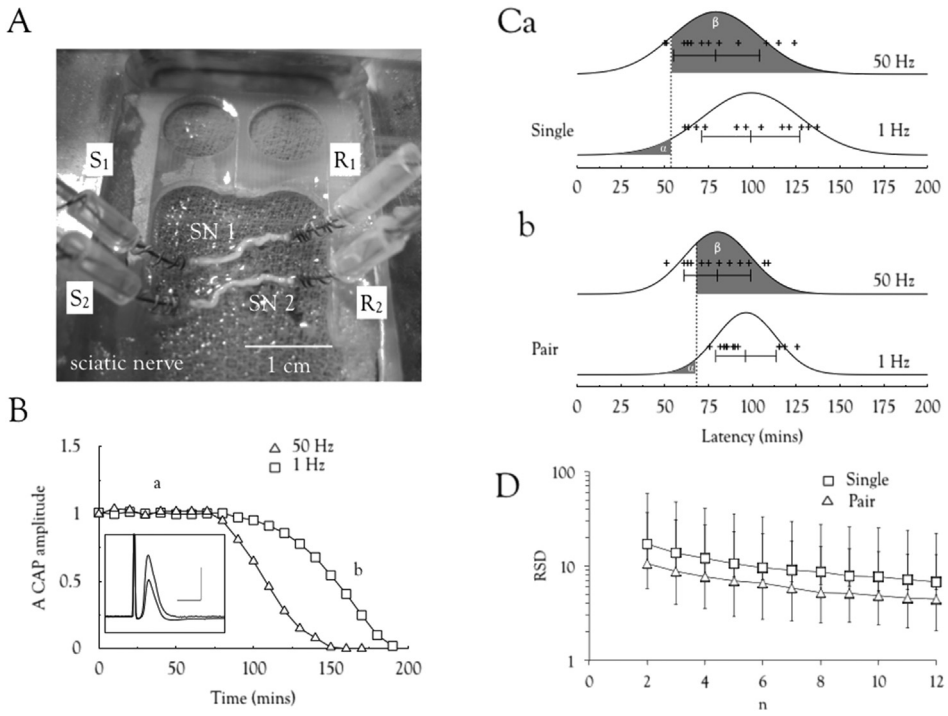

Figure 3. Recordings of the A fibre sciatic nerve CAP exposed to aglycaemia. A. Experimental set up illustrating simultaneous recording of the CAPs from a pair of sciatic nerves, showing placement of stimulating electrodes (S_1 and S_2), recording electrodes (R_1 and R_2) relative to the sciatic nerves (SN 1 and SN 2). B. The amplitude of the sciatic nerve A fibre CAP plotted against time, where aglycaemia was introduced at 0 min. The latency to CAP failure to 95% of baseline was quickest in nerves stimulated at 50 Hz compared to nerves stimulated at 1 Hz. Inset shows individual A fibre CAPs recorded at the time points a and b. Scale bar is 1 ms and 2 mV. C. Plotting the data as normal distributions where the sample means and standard deviations determine the distribution profiles (a). Upper traces show that imposing 50 Hz at the onset of aglycaemia accelerates latency to CAP failure compared to stimulating at 1 Hz in recordings from single nerves (b). The lower traces show similar data but for recordings from pairs of nerves. Note how the area of β is smaller for the recordings from pairs of nerves at 50 Hz compared to single nerve recordings. The mean and standard deviation are indicated by the vertical bars. Individual data points are denoted by crosses (also applies to Figure. 4C). D. The RSD calculated from recordings from either single or pairs of nerves stimulated at 1 Hz is lower for pairs of nerves than for single nerves for equivalent values of n.

showing the RSD for sciatic nerves stimulated at 1 Hz for recordings from single or pairs of nerves (Figure 3D). For each value of n, the estimate of the RSD was calculated using an empirical bootstrapping technique (see Methods). As expected, S (and accordingly RSD) decreased as n increased. Importantly, RSD is consistently higher for single nerves than for nerves that are paired. This decrease in the value of S from recordings from pairs of nerves results in the *critical value* moving closer to the mean for nerves stimulated at 1 Hz, with a correspondingly smaller value of β for the nerves stimulated at 50 Hz, and hence increased Power (compare the upper and lower 50 Hz traces in Figure 3C).

As a test of the cross-preparation validity of the hypothesis that recording from pairs of nerves reduces the random error for equivalent n values compared with recordings from single nerves, we investigated the ability of glycogen to support axon conduction in a series of experiments in mouse optic nerve (MON). A similar recording set up was used as described for the sciatic nerves (see above), where two separate sets of

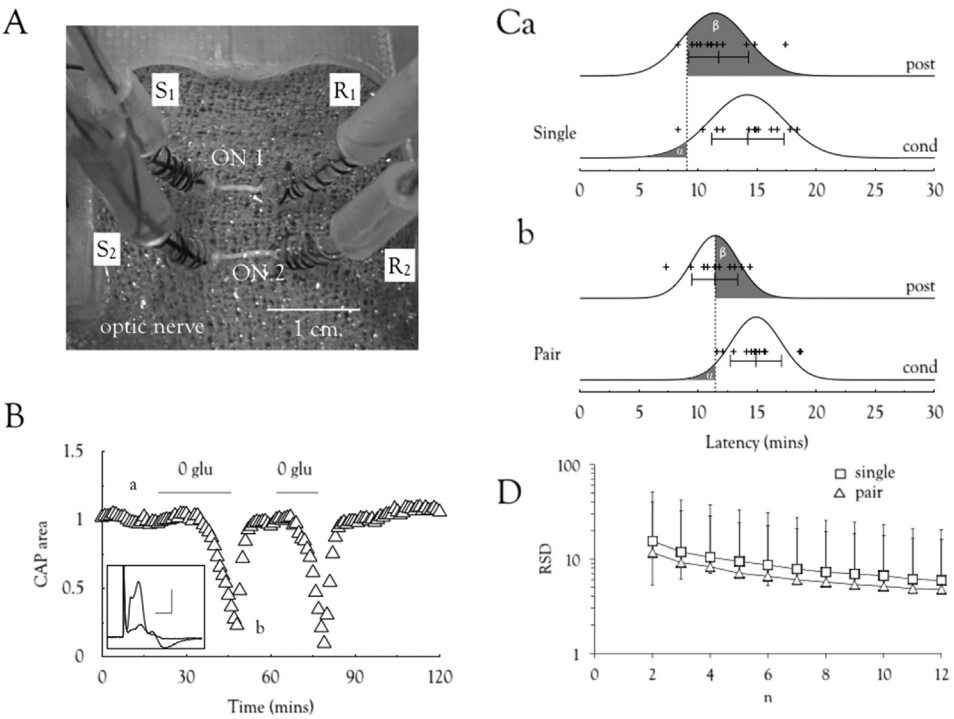

Figure 4. Recordings of the MON CAP exposed to repeated aglycaemia. A. Experimental set showing simultaneous recording of the CAPs from a pair of MONs, showing placement of stimulating electrodes (S_1 and S_2) and recording electrodes (R_1 and R_2) relative to the MONs (SN 1 and SN 2). B. The area of the MON CAP plotted against time, where periods of aglycaemia are denoted by the horizontal bars. Inset shows representatives examples of the CAP recorded at time points a and b. Scale bar is 1 ms and 2 mV. C. Plotting the data as normal distributions where the sample means and standard deviations determine the distribution profiles (a). Upper traces show that the latency to CAP failure from recordings of single MONs during the post-conditioning period (post) of aglycemia is accelerated compared to the conditioning period (b). The lower traces show similar data but for recordings from pairs of nerves. Note how the area of β is smaller for post conditioning recordings from pairs of nerves compared to single nerve recordings. D. The RSD calculated from recordings from either single or pairs of nerves during the preconditioning period of aglycaemia is lower for pairs of nerves than for single nerves for equivalent values of n.

experiments were carried out, one on single nerves and the other on pairs of nerves. The set up where CAPs from pairs of optic nerves were simultaneously recorded is illustrated (Figure 4A). In these experiments the MON was exposed to aglycaemia, the conditioning period, until the CAP started to fail. When the CAP had fallen to about half of its baseline area control aCSF containing 10 mM glucose was reintroduced and the CAP began to recover. After the CAP had fully recovered aglycaemia was again introduced, the post-conditioning period (Figure 4B). The reasoning behind this protocol is that glycogen will support the CAP during the conditioning period of aglycemia, but there is insufficient time for glycogen to be replenished before the post-conditioning period of aglycemia (Brown et al., 2003), hence the latency to CAP failure should be accelerated after the post-conditioning period of aglycaemia compared to the conditioning period. Displaying the data as normal distributions (Figure 4C) as described above for the sciatic nerve data reveals that in recordings from single nerves the latency to CAP failure resulting from the conditioning period of aglycaemia was 14.2 ± 3.1 min, whereas it was 11.4 ± 2.7 min ($n = 12$) post-conditioning. CAP recordings from pairs of nerves resulted in similar values for the means but the standard deviation was decreased (14.9 ± 2.1 versus 11.5 ± 1.9 min; $n = 12$). There was no significant difference between the conditioning or post-conditioning value of the means recorded singly or in pairs ($p = 0.6$, $p = 0.5$), but the p values (t-test: two sample uneven variance) fell from 0.015 in single experiments to 0.001 in pairs of nerve experiments, reducing the chance of making a Type I error, as a consequence of the decrease in RSD exhibited by the recordings from pairs compared to single nerves (Figure 4D).

5. Discussion

This paper is a natural progression from a recent study in which we described a method whereby A and C fibre CAPs could be recorded simultaneously from a single sciatic nerve via judicious use of a two channel stimulator, exploiting the differences in recruitment threshold of the two fibre types, thereby reducing the number of animals used to obtain an equivalent number of datasets (Rich and Brown, 2018). We demonstrate the mathematical reasoning behind our hypothesis of increased experimental efficiency i.e. maintaining the effect size without altering the magnitude of Type I or Type II errors, whilst decreasing the sample size. This allows us to reduce the number of animals used in experiments on *ex vivo* acutely isolated sciatic and optic nerve without compromising the statistical Power of the study, and is in accord with the National Centre for Replacement, Refinement and Reduction in Animal Experiments in the UK.

5.1. Glycogen

In sciatic nerves exposed to aglycaemic conditions, the A fibre CAP began to fail after about 100 min when stimulated at 1 Hz. Additional 50 Hz stimulus during aglycaemia accelerated latency to CAP failure to about 80 min. Thus there is an enormous disparity between the numbers of action potentials experienced between the two conditions and the relatively small acceleration in latency to CAP failure in nerves exposed to 50 Hz, suggesting that the energy required to re-equilibrate ion gradients in the face of 50 Hz stimulus is not great. These data are in agreement with similar MON experiments, which demonstrated accelerated CAP failure when exposed to high frequency stimulation, supporting a role for glycogen in maintaining CAP conduction in aglycaemic conditions (Brown et al., 2003). The greater the tissue energy demand, the faster the consumption of glycogen. In MONs exposed to aglycaemia the latency to CAP failure is about 15 min (Brown et al., 2003), but pre-depleting glycogen with a conditioning period of aglycaemia caused an accelerated CAP failure since the absence of glycogen promotes CAP failure.

5.2. Failure rate

An unavoidable feature of electrophysiological recordings in which tissue is acutely dissected from experimental animals and transferred to a recording chamber, is that not every nerve will yield a viable recording, i.e. the technique is accompanied by a perceptible failure rate, which reflects the capricious nature of delicate, vulnerable tissue that is exquisitely sensitive to mishandling. Based on probability theory (De Muth, 2006) we can estimate the number of successful experiments, i.e. those that produce viable recordings as:

$$v = n \times m \times p^m \tag{4}$$

where v is the number of viable nerve recordings, n is the number of mice used, m denotes whether a single nerve or a pairs of nerves are used and is allocated a value of 1 or 2, respectively, and p is the probability of a successful recording from a nerve (the complement of failure rate), whose values covers the range 0–1, where 0 signifies no successful experiments and 1 denotes success in all experiments. The relationship is illustrated graphically in Fig 5A, B, which demonstrates an extremely important principle related to the tenet of the 3Rs, namely the reduction in animal use. At a probability of success greater than 50% when employing an n of 10, recordings from pairs of nerves produced more viable experiments than recordings derived from single nerves. An alternative way of representing this relationship is to determine how may animals are required to produce a certain number of viable experiments for a given probability of success (Figure 5B), and again indicates that a $p > 0.5$ is required for recordings from pairs of nerves to be justified based on number of animals used. We ascribe our routine success rate in excess of 90% to careful dissection of tissue, which we have described in detail elsewhere (Rich and Brown, 2018).

5.3. Critical value relies on the normal distribution irrespective of sample size

Given the rigid foundation upon which statistical analysis is based it is surprising to find an obvious anomaly in Power calculations; the estimate of the significance level uses *critical values* based on the normal distribution irrespective of the value of n. The effect on the *critical value* can be appreciated by consulting Figure 5, which shows how the t value of the Student's distribution varies for α levels of between 0.01 and 0.1 according to sample size (Figure 5C, D). At an α level of 0.05 the t value is significantly increased for lower values of n (e.g. for $n = 3$, t approaches double the value for the normal distribution, Figure 5C), which would lead to increased estimates of β and decreased Power. The reason for this anomaly lies in the relationship whereupon the value of t depends on n, which in turn depends on t, thus for each iteration of n the *critical value* changes. Prior to the ubiquitous presence of desktop computers this double iteration involved in using the Student's t distribution would have proved too unwieldy for practical purposes. For values of n greater than 30 the discrepancy from the real value of t is small (Kachigan, 1991) and a pragmatic view has been adopted by most researchers, summarised by the opinion that "I don't think the discrepancy is worth worrying about, because the calculations are based on an estimated value of the standard deviation and are only supposed to calculate an estimated sample size." (Motulsky, 1995).

5.4. Additional cost

The technique does require additional equipment in the form of a stimulator and an amplifier to acquire the stimulus evoked CAP from the second nerve. Although multiple channel stimulators are available, such as the Grass S88 that we use, most laboratory stimulators are single channel and cannot stimulate two nerves simultaneously in a controllable

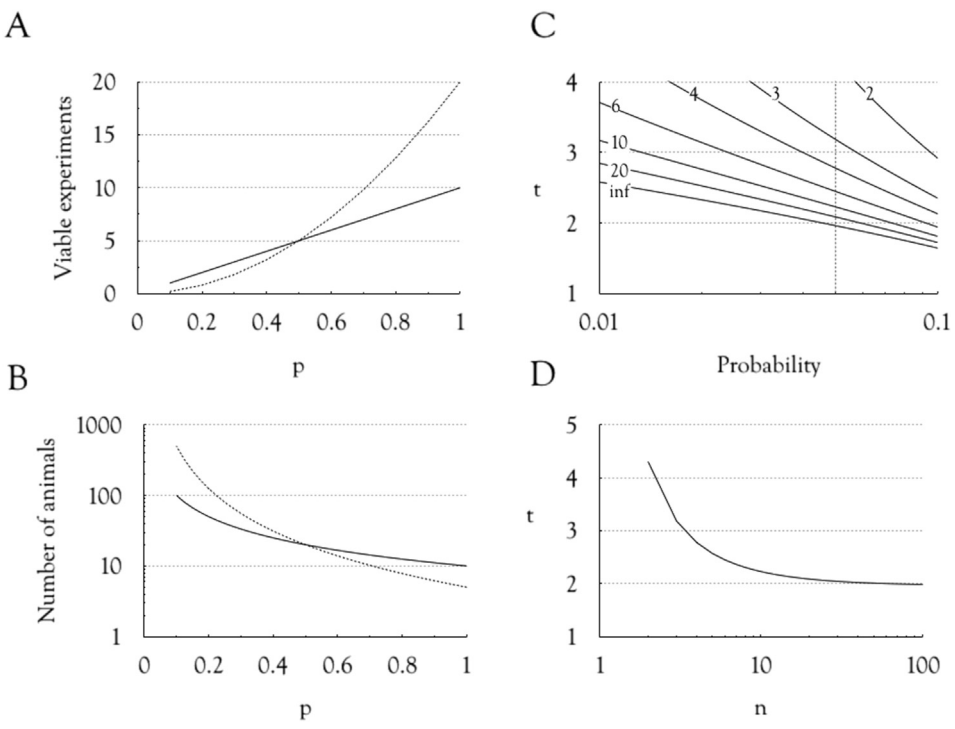

Figure 5. The number of viable experiments relative to the success rate. A. The number of viable experiments is calculated for both single and pairs of experiments from 10 mice. As the probability of experimental success increases so does the number of viable experimental resulting from recordings from single (bold line) and pairs of nerves (dotted line) based on Eq. (4). However the success rate increases linearly for single nerves, but as a power function for pairs of nerves, such that at success probabilities of greater than 50% the number of viable experiments for pairs of nerves exceeds that for single nerves. B. The number of animals required to produce 12 viable recordings as a function of probability. Recordings from single (bold line) and pairs of nerves (dotted line) according to Eq. (4). C. The critical value of the Student's t distribution (t) relative to the probability for defined values of n, calculated using the tinv function in Excel. At $p = 0.05$ note the steep increase in t as the value of n decreases. D. The value of t for n of 2–100 at $p = 0.05$, showing the steep increase in t for $n < 10$. As the value for n increases t approaches the normal distribution (1.96) justifying the use of the standard deviation as an estimate of σ for $n > 30$.

manner. However battery operated stimulators and amplifiers are relatively cheap and savings derived from reduced animal use would quickly recoup the cost.

5.5. Replication and sources of error

In order for a nerve to constitute a sample and increase the value of n it must meet three distinct criteria (Lazic et al., 2018). These are (1) that the mice must be independently randomised to treatment conditions, (2) the treatment must be independently applied to each nerve, and must not affect other nerves, and (3) the nerves must not influence each other. In our experiments the mice were randomised to either 1 Hz or 50 Hz stimulus, the nerves were removed and placed in the bath, then the treatment was applied, and when the nerves were in the bath they did not influence other nerves. In this study we recorded from nerves from an in-bred strain of mouse, which, while not technically clones, have been bred specifically to be as similar as possible, although strains are inevitable susceptible to spontaneous mutations (Enríquez, 2019). This facilitates our explicit intention, which is to be confident that any differences we record experimentally can be presumed to arise from real differences resulting from a physiological or pathological process and not as a result from variation in the phenotypic properties of the nerves.

There are two types of error associated with experimental measurement, random and systematic (De Muth, 2006; Hinton, 2004). Random errors arise from unpredictable changes and can be described by a normal distribution, where the standard error of the mean is an estimate of the random error associated with the experimental measurement. Systematic errors are reproducible inaccuracies that are associated with faults in recording and are unpredictable in nature. It is the random error that we are aiming to reduce by using pairs of nerves for recordings. The random nature of our experimental recording environment means that variables such as temperature, chamber oxygenation, dissection, aCSF composition, nerve diameter relative to suction electrode size etc. can affect the precision of the results (De Muth, 2006). Our reasoning is that when recording from pairs of nerves simultaneously the effect of these variables will be reduced, since each pair of nerves will be exposed to identical experimental conditions, thus reducing random errors. The reduction in RSD in recordings from pairs of nerves compared to single nerve recordings indicates that we have been successful in this endeavour. We recognise that our technique of decreasing random error elevates the risk of increasing the systematic error. Since systematic is continuously monitored and controlled throughout all experiments, we believe this trade-off generates a net benefit to the power of the study.

6. Conclusions

Recordings from pairs of nerves simultaneously has allowed us to reduce the number of mice used in experiments designed to test the role of glycogen in supporting axonal conduction during periods of aglycaemia in both sciatic and optic nerve. Mathematical analysis of our data showed that for equivalent number of nerves, when recordings derived from paired recordings the p value of comparisons was lower and power was higher meaning that under these conditions the risk of making Type I and Type II error was reduced compared to recordings from single nerves. The effects that we describe i.e. using pairs of nerve to reduce variability whilst maintaining statistical Power, can be viewed as a procedure that could be generally applied to other experimental scenarios unrelated to the metabolic studies we describe.

Declarations

Author contribution statement

Laura R Rich: Performed the experiments; Analyzed and interpreted the data.

Jonathan A. Patrick: Analyzed and interpreted the data; Contributed reagents, materials, analysis tools or data.

Margaret A Hamner: Performed the experiments.

Bruce R Ransom: Conceived and designed the experiments; Contributed reagents, materials, analysis tools or data.

Angus M Brown: Conceived and designed the experiments; Performed the experiments; Analyzed and interpreted the data; Contributed reagents, materials, analysis tools or data; Wrote the paper.

Funding statement

This work was supported by the Biotechnology and Biological Sciences Research Council (Grant Number BB/M008770/1) via a BBSRC DTP.

Competing interest statement

The authors declare no conflict of interest.

Additional information

No additional information is available for this paper.

Acknowledgements

We thank Robert Humphrey for useful discussions on pseudoreplication.

References

Baker, M., Bostock, H., Grafe, P., Martius, P., 1987. Function and distribution of three types of rectifying channel in rat spinal root myelinated axons. J. Physiol. 383, 45–67.

Bernstein, S.L., Bernstein, R., 1999. Elements of Statistics II: Inferential Statistics. McGraw Hill, New York.

Brown, A.M., 2006. A non-linear regression analysis program for describing electrophysiological data with multiple functions using Microsoft Excel. Comput. Methods Progr. Biomed. 82, 51–57.

Brown, A.M., Evans, R.D., Black, J., Ransom, B.R., 2012. Schwann cell glycogen selectively supports myelinated axon function. Ann. Neurol. 72, 406–418.

Brown, A.M., Tekkok, S.B., Ransom, B.R., 2003. Glycogen regulation and functional role in mouse white matter. J. Physiol. 549, 501–512.

Brown, A.M., Wender, R., Ransom, B.R., 2001. Metabolic substrates other than glucose support axon function in central white matter. J. Neurosci. Res. 66, 839–843.

Cummins, K.L., Perkel, D.H., Dorfman, L.J., 1979. Nerve fiber conduction-velocity distributions. I. Estimation based on the single-fiber and compound action potentials. Electroencephalogr. Clin. Neurophysiol. 46, 634–646.

Curran-Everett, D., 2009a. Explorations in statistics: hypothesis tests and P values. Adv. Physiol. Educ. 33, 81–86.

Curran-Everett, D., 2009b. Explorations in statistics: the bootstrap. Adv. Physiol. Educ. 33, 286–292.

De Muth, J.E., 2006. Basic Statistics and Pharmaceutical Statistical Applications, second ed. ed. Chapman & Hall, Boca Raton.

Edgar, J.M., McCulloch, M.C., Montague, P., Brown, A.M., Thilemann, S., Pratola, L., Gruenenfelder, F.I., Griffiths, I.R., Nave, K.A., 2010. Demyelination and axonal preservation in a transgenic mouse model of Pelizaeus-Merzbacher disease. EMBO Mol. Med. 2, 42–50.

Edgar, J.M., McLaughlin, M., Werner, B., Malis, C., McCulloch, C., Barriel, J.A., Brown, A.M., Faichney, A.B., Snaideron, N., Nave, K.-A., Griffiths, I.A., 2009. Early ultrastructural defects of axons and axon-glia junctions in mice lacking expression of CNP1. Glia 57, 1815–1824.

Enríquez, J.A., 2019. Mind your mouse strain. Nat. Metabol. 1, 5–7.

Fern, R., Waxman, S.G., Ransom, B.R., 1994. Modulation of anoxic injury in CNS white matter by adenosine and interaction between adenosine and GABA. J. Neurophysiol. 72, 2609–2616.

Hamner, M.A., Moller, T., Ransom, B.R., 2011. Anaerobic function of CNS white matter declines with age. J. Cerebr. Blood Flow Metabol. 31, 996–1002.

Hamner, M.A., Ye, Z., Lee, R.V., Colman, J.R., Le, T., Gong, D.C., Ransom, B.R., Weinstein, J.R., 2015. Ischemic preconditioning in white matter: magnitude and mechanism. J. Neurosci. 35, 15599–15611.

Hinton, P.R., 2004. Statistics Explained, second ed. ed. Routledge, London.

Kachigan, S.K., 1991. Multivariate Statistical Analysis. Radius Press, New York.

Kocsis, J.D., Gordon, T.R., Waxman, S.G., 1986. Mammalian optic nerve fibers display two pharmacologically distinct potassium channels. Brain Res. 383, 357–361.

Lazic, S.E., Clarke-Williams, C.J., Munafo, M.R., 2018. What exactly is 'N' in cell culture and animal experiments? PLoS Biol. 16, e2005282.

Motulsky, H., 1995. Intuitive Biostatistics. OUP, Oxford.

Patton, H.D., 1982. Special properties of nerve trunks and tracts. In: Ruch, T., Patton, H. (Eds.), Physiology and Biophysics: IV Excitable Tissues and Reflex Control of Muscle. W.B. Saunders Company, Philadelphia, pp. 101–127.

Ransom, B.R., Fern, R., 1997. Does astrocytic glycogen benefit axon function and survival in CNS white matter during glucose deprivation? Glia 21, 134–141.

Rich, L.R., Brown, A.M., 2018. Fibre sub-type specific conduction reveals metabolic function in mouse sciatic nerve. J. Physiol. 596, 1795–1812.

Sokal, R.R., Rohlf, F.J., 1995. Biometry, third ed. W.H. Freeman and Company, New York.

Stys, P.K., Ransom, B.R., Waxman, S.G., 1991. Compound action potential of nerve recorded by suction electrode: a theoretical and experimental analysis. Brain Res. 546, 18–32.

Stys, P.K., Ransom, B.R., Waxman, S.G., 1990. Effects of polyvalent cations and dihydropyridine calcium channel blockers on recovery of CNS white matter from anoxia. Neurosci. Lett. 115, 293–299.

Stys, P.K., Waxman, S.G., Ransom, B.R., 1992. Ionic mechanisms of anoxic injury in mammalian CNS white matter: role of Na^+ channels and Na^+-Ca^{2+} exchanger. J. Neurosci. 12, 430–439.

Wang, Q., Vlkolinsky, R., Xie, M., Obenaus, A., Song, S.-K., 2012. Diffusion tensor imaging detected optic nerve injury correlates with decreased compound action potentials after murine retinal ischemia. Invest. Ophthalmol. Vis. Sci. 53, 136–142.

Wender, R., Brown, A.M., Fern, R., Swanson, R.A., Farrell, K., Ransom, B.R., 2000. Astrocytic glycogen influences axon function and survival during glucose deprivation in central white matter. J. Neurosci. 20, 6804–6810.